

## Automated high resolution ectoenzyme measurements: instrument development and deployment in three trophic regimes

Brian M. Gaas\* and James W. Ammerman

Institute of Marine and Coastal Sciences, Rutgers University, New Brunswick, New Jersey 08901

### Abstract

A commercial flow-injection analysis (FIA) unit was adapted for rapid, automated measurements of ectoenzyme activity. Seawater was injected with a small amount of the substrate 6,8-difluoro-4-methylumbelliferyl phosphate or L-leucine-7-amido-4-methylcoumarin, the hydrolysis products of which were measured fluorometrically in a flow cell. The FIA system was run using sequential injection stopped-flow analysis, allowing activities to be calculated directly from the rate of substrate hydrolysis. The FIA unit sampled autonomously, with the exception of running standard curves and creating new killed controls. The FIA unit was deployed in three environmentally distinct locations – the hypereutrophic Louisiana shelf (July 2004), the oligotrophic Sargasso Sea (February–March 2005), and the eutrophic Hudson River estuary (April 2005). Both phosphatase (Louisiana shelf and Sargasso Sea cruises) and peptidase (Hudson estuary cruise) activities were detectable by the FIA unit. Good correlations were observed between activities measured by the FIA unit and a fluorescence microplate reader. Incubation times ranged from 5–20 min with sampling rates of one sample every 11–26 min. Differences in incubation time, mixing coil length, and detector settings altered the dilution of standards and substrates but did not affect the detection limit of fluorescence. High resolution contour maps and time-series measurements of ectoenzyme activities in eddies, localized upwellings and downwellings, blooms, and river plumes may be used to understand and predict biogeochemical changes in these and other aquatic environments.

Ectoenzymes are a class of hydrolase that operates on or near the cell surface or in the periplasmic space (Martinez and Azam 1993). This definition is used to distinguish ectoenzymes from intracellular enzymes which reside within the cytoplasm and extracellular enzymes which are not associated directly with the cell (Chrost and Siuda 2002). Much of the available organic matter required by microbes is too large for direct transport into the cytoplasm. Ectoenzymes are used by the cell to convert large and polymeric molecules into smaller, transportable products. This activity plays a major role in dis-

solved organic matter transformations in both surface and deep waters and can be used to determine dissolved organic matter use (Stepanuskas et al. 1999). By extension, enzyme activities also are linked to important topics such as global carbon cycling. Two frequently measured classes of ectoenzymes are phosphatases (which cleave phosphate monoesters) and peptidases, which cleave peptide bonds (Chrost 1991). Certain ectoenzymes, such as alkaline phosphatase (AP), can be used as potential identifiers of nutrient limitation in the environment, in association with bioavailable nutrient concentrations (Soderstrom 1996; Hoppe 2003), nutrient ratios (Jarvinen et al. 1999), and biological response (Beardall et al. 2001).

A routine ectoenzyme assay uses the hydrolysis of an ectoenzyme substrate and subsequent production of a fluorescent compound to measure activity (Hoppe 1993). High fluorescence yield and low background fluorescence will increase assay sensitivity (Ammerman and Glover 2000). Previous enzyme activity measurements have used incubation times ranging from a few hours to multiple days in oligotrophic regions (Perry 1972; Christian and Karl 1995; Taylor et al. 2003; Kirchman et al. 2004; Sebastian et al. 2004). Although increasing incubation time does not affect the detection limit of fluorescence (there is no change in the quantum yield of

\*Corresponding author: Phone: (732) 932-6555. Fax: (732) 932-8578. E-mail: gaas@marinc.rutgers.edu

### Acknowledgments

Many thanks are needed for people who supported this work: Garth Kline of Fialab, Inc. for technical assistance, Jason Sylvan for microplate reader processing, and Stephanie Jaeger for insightful suggestions and more microplate reader work. Bob Chant and Mike Lomas provided opportunities to test EAAS in the Hudson River and Sargasso Sea and ancillary data in these regions. Further thanks go out to the crews of the R/V Pelican and R/V Oceanus. Credit also goes to three anonymous reviewers who certainly improved the quality and readability of this manuscript. Funding for this project came from NSF (OCE 0196175 – Biological Oceanography, Ocean Technology and Interdisciplinary Coordination; DBI 0216154 – Biocomplexity), and NOAA CSCOR (NA03NOS4780041) grants to J.W.A.

the fluorescent compound), it does allow lower activities to be measured.

Two main types of instruments currently are used for enzyme activity measurements with fluorescent substrates (Ammerman and Glover 2000; Marx et al. 2001; Huston and Deming 2002; Sylvan et al. 2007): 1) manual fluorimeters, and 2) fluorescence microplate readers. Assays done manually or using a microplate reader require the user to manipulate the sample at both the sample acquisition and substrate additions steps. In manual assays, temporary deviations from linearity (from settling particles or dispersion) may be difficult to identify due to discontinuous measurements and constant handling. A fluorescence microplate reader can run multiple samples and/or enzymes at the same time, including replicates. Incubation times are preset with automated measurements and data logging, providing more freedom for the experimenter. However, the delay between sample acquisition and measurement may lead to changes in activity.

A previous continuous-flow method was used to automate fluorescence ectoenzyme activity measurements (Ammerman and Glover 2000). This shipboard system was used successfully in the high-activity waters of the Louisiana shelf. However, the configuration of incubation coils and mixing lines made the described system cumbersome for routine use. In addition, the use of continuous-flow for enzyme activity measurements mandates stable background fluorescence, a condition which required frequent operator intervention.

FIA has been in use as an analytical technique for ~30 years (Ruzicka 2000) and is applied to chemical (colorimetric), pharmaceutical, and environmental assays (Chen and Ruzicka 2004). With appropriate computer controls and hardware, sample uptake, reagent/substrate mixing, incubation timing, and measurement, all can be automated. The reproducibility of sample processing is one of the largest advantages of an FIA system for measurements, especially in comparison to manual and microplate-based enzyme assays (Ruzicka 2000). FIA-based fluorometry has been used previously as a sample delivery system for fluorescence ectoenzyme measurements, only after separate external incubations, however (Delmas et al. 1994; Delmas and Garet 1995).

Ectoenzyme activity is directly related to organic matter use and also can be associated with biomass, nutrient turnover rates, and potential nutrient limitation. Continuous ectoenzyme measurements begin to approach the rates of temperature, salinity, and fluorescence measurements made on research vessels. Fine-scale resolution is available with an automated system, which may allow detailed comparisons to be made between enzyme activity and environmental parameters. This manuscript describes the development of the Enzyme Activity Analysis System (EAAS), an automated sequential injection stopped-flow FIA protocol for the measurement of aquatic ectoenzyme activity. Details on the hardware configuration, plumbing, and data processing are provided, as well as the ability of the machine to measure ectoenzyme activities in

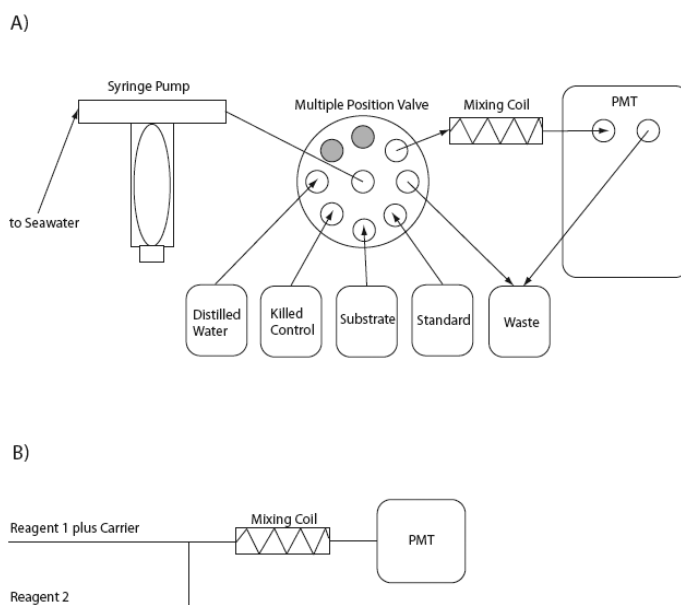


**Fig. 1.** EAAS schematic of plumbing configuration. A) Schematic of fluid flow. The direction of the arrows represents the direction of fluid flow during normal sampling. The line connecting the syringe pump to the multiple position valve accepts fluids in both directions, depending on whether EAAS is aspirating reagents toward the syringe or pushing fluid toward the detector. Grey ports in multiple position valve were not used. B) Fluid wiring diagram. The following analytes are created by switching Reagent 1 (R1) and Reagent 2 (R2): standard curve (R1 = distilled water, R2 = standard), substrate baseline (R1 = distilled water, R2 = substrate), sample (R1 = seawater, R2 = substrate), killed control (R1 = killed control, R2 = substrate), internal standard (R1 = seawater, R2 = standard).

various natural marine environments – the hypereutrophic Louisiana shelf, oligotrophic Sargasso Sea, and eutrophic Hudson River estuary.

## Materials and procedures

**EAAS Operations**—A commercial flow-injection machine (Fialab 3500B) from FIALabs, Inc was used for the development of the Enzyme Activity Analysis System (EAAS). The flow diagram is shown in Fig. 1. The machine had a glass 5 mL, 24,000-step syringe pump (Cavro), a four-channel bidirectional peristaltic pump, and an eight-port multiple position valve. The peristaltic pump was not used in our design. EAAS was controlled by a laptop computer (Dell Latitude D800, Windows XP) running the supplied WinFIA v5.0 software that directed the fluid flow, light source, detector, and data storage. The light source was a high output light emitting diode (LED) with peak emission at  $375 \text{ nm} \pm 12 \text{ nm}$ . The LED was rewired to the Fialab 3500B internal 12V power cable via a double pole/double throw relay, allowing the computer to turn the LED on and off. The holding line was 57 cm of non-coiled 0.762 mm internal diameter (i.d.) polyetheretherketone (PEEK) tubing. All reagents were aspirated through Teflon tubing of 0.508 mm i.d. The same type of tubing was used in the

mixing coil to link the multiple position valve to the detector. The initial mixing coil length was 71 cm (Louisiana Shelf and Sargasso Sea) and was later shortened to 66 cm (Hudson estuary). All tubing was connected by Upchurch fittings. Fluorescence was measured in a 3 mm path length quartz flow cell with a 100  $\mu\text{L}$  volume (Helma). The detector was a photomultiplier tube (PMT) with  $365/500 \pm 15$  nm excitation/emission filters, respectively, corresponding to the absorbance/emission spectra of the fluorescence standards 6,8-difluoro-4-methylumbelliferone (dfMUF, from Invitrogen) or 7-amido-4-methylcoumarin (AMC, from Sigma) of 365/460 nm. The PMT took readings at 2 Hz, 100 msec integration time (Louisiana shelf) and 0.5 Hz, 200 msec integration time (Sargasso Sea and Hudson estuary). Differences in expected activity between the hypereutrophic Louisiana shelf (very high activity), oligotrophic Sargasso Sea (very low activity), and eutrophic Hudson River estuary (moderate to high activity) dictated the incubation and integration time and, in part, tubing length.

EAAS used five different types of solutions. Seawater (carrier and enzyme source) was acquired on the Louisiana shelf cruise through a sampling arm suspended 6 m from the port side of the ship to sample water from <1 m depth. The Sargasso Sea and Hudson estuary cruises sampled from the ship's uncontaminated seawater system, originating at the bow at a depth of  $\sim 2.5$  m. Salinity readings were simultaneously acquired through the ship's salinometer, with a sampling rate of approximately  $1 \text{ min}^{-1}$  on all the cruises. Killed controls were seawater samples boiled twice via microwaving with an ice bath cooling after each and were used in place of non-killed seawater in sample runs (i.e., as both the carrier and enzyme source). Ultra-pure Milli-Q water (18.2 M $\Omega$ ), used for washing and as a solvent in standard and substrate solutions, was boiled twice via microwaving with an ice bath cooling after each. External standards of 0, 250, 500, 1000, and 2000 nM pre-dilution concentrations were created using the boiled distilled water as the primary solvent. A 100  $\mu\text{M}$  solution of AP substrate and 200  $\mu\text{M}$  solution of peptidase substrate, both pre-dilution, were created using 6,8-difluoro-4-methylumbelliferyl phosphate (dfMUF-P, from Invitrogen) and L-Leucine-7-amido-4-methylcoumarin (Leu-AMC, from Sigma), respectively. Both solutions were produced using boiled and cooled distilled water as the primary solvent. The substrates were kept constantly in a dark, insulated ice bath.

In order to maximize the fluorescence signal, the entire reaction bolus (substrate injection plus the seawater the substrate disperses into) should be present in the flow cell at the time of measurement. Localization of the reaction bolus within the cuvette was achieved by running a 10  $\mu\text{L}$  injection of fluorescent standard slowly through EAAS in a continuous-flow method. The volume of carrier required to reach maximal fluorescence was assumed to equate to maximal localization and subsequently used for sample measurements.

EAAS runs consisted of 20, 50, or 100 samples, depending on the rapidity of visible detritus accumulation in the syringe;

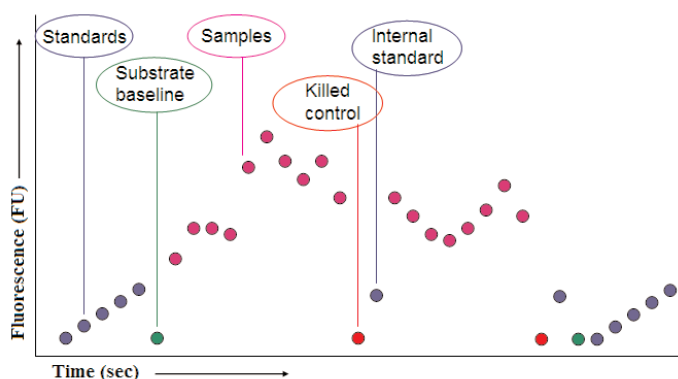


**Fig. 2.** EAAS sampling sequence. The run begins with a five-point standard curve. This is followed by measurement of unhydrolyzed substrate in distilled water to measure background fluorescence. A series of ten samples followed by one killed control and one internal standard is repeated multiple times during the run. The internal standard is an identical injection of the fifth standard in the standard curve, used to monitor instrument drift and carry-over through the run. At the end of the run, a second substrate in distilled water injection is compared with the first to monitor substrate autolysis. The run ends with a second five-point standard curve.

faster accumulation required more frequent instrument cleaning to prevent clogging and hence had fewer samples per run. Each run followed the same progression: a five-point external standard curve, substrate baseline, a repeating series of ten samples with one internal standard and one killed control (a series was always ten samples, one internal standard and one killed control), a second substrate baseline, and a second five-point external standard curve (Fig. 2). Prior to each EAAS run, the substrate and standard lines were primed by aspirating enough solution to fill the corresponding lines, with excess being injected out the waste line. A substrate baseline was produced through a 10  $\mu\text{L}$  injection of substrate into a distilled water carrier, used to monitor substrate autolysis. Internal standards were repetitions of the 2000 nM standard (pre-dilution concentration) in distilled water. The internal standard provided an indicator of washing efficiency, in so far as insufficient washes could lead to an increase in internal standard fluorescence over time. Interpolation between internal standards also provided mid-run corrections to the standard curve. A full run (20, 50, or 100 samples) was followed by 10–20 flushes of 5 mL distilled water through each line. The speed of these flushes varied from 100–200  $\mu\text{L min}^{-1}$ . When the syringe pump accumulated visible matter or discoloration, as well as after every two runs, a 10% HCl solution was flushed through the system (20 flushes using 5 mL through each line) to prevent clogging of the small diameter tubing. As material seemed limited to the syringe, and substrate was not added to fluid within the pump, the influence of matter accumulation on activity was likely limited.

For each sample or standard, 5.0 mL water (distilled water for standards, seawater for samples) were aspirated. The syringe emptied 2.5 mL ( $\sim 5$  times the volume of the detection

line plus cuvette) along the sample path to fill the system with new water. A 10  $\mu\text{L}$  bolus of substrate or standard was aspirated at 50  $\mu\text{L sec}^{-1}$  into the holding line and moved to the flow cell at 20  $\mu\text{L sec}^{-1}$  by the carrier stream water obtained during the original 5.0 mL aspiration. There was a 1 min delay between the reaction mixture entering the flow cell and recording the PMT data in a stopped-flow method. The reaction occurring between the seawater carrier and the injected substrate was monitored for either 5 min (Louisiana shelf and Hudson estuary) or 20 min (Sargasso Sea). The remaining  $\sim 2$  mL of water in the syringe were used to flush out the flow cell. For samples, three further washes using 5 mL each of distilled water were used to flush out the sample intake/detector lines and syringe of salts and accumulated materials. Individual standards were separated by two washes of 5 mL each. Depending on the speed of the flushing, these volumes and flow rates resulted in a sample processing time of 6–9 min plus the length of the incubation (i.e., 11 min for the Louisiana shelf, 14 min for the Hudson estuary, 26 min in the Sargasso Sea).

**Activity calculations**—Maximal fluorescence is decreased through dilution with the carrier, a necessary result of using the carrier as a reagent (the enzyme source). The degree of dilution was quantified as a dilution factor, the ratio of the fluorescence of a bolus of undiluted standard (the cuvette filled entirely with the standard solution) to the fluorescence of a bolus of standard measured by EAAS using normal sampling parameters. Volumetric consideration between the substrate/standard injection (10  $\mu\text{L}$ ) and cuvette (100  $\mu\text{L}$ ) imparts a minimum dilution factor of 10. Higher dilution factors are indicative of the degree of mixing and/or incomplete sequestration of the injection bolus within the flow cell. The dilution factor was used to correct the concentrations of the standards for activity calculations.

Activity was calculated as  $\text{Activity} = \text{Sample Slope} / \text{Standard Slope} \times 3600$  (units:  $\text{nmol L}^{-1} \text{hr}^{-1}$ ). The initial standard slope was calculated from a least-squares linear regression of the first standard curve (units: fluorescence units [FU]  $\text{nmol L}^{-1}$ ). For each internal standard, an intermediate standard slope was calculated based on the difference in fluorescence between the internal standard and 0 nM standard. Standard slopes for each sample time were derived through linear interpolation between the standard curves and internal standards. In addition, all standard slope calculations were corrected for dilution. The slope of the sample fluorescence change was calculated as a linear regression of FU and time (units:  $\text{FU sec}^{-1}$ ). To prevent errors from slope changes due to diffusion during measurement, only the final one-third of the data points were used in slope calculations. Negative activities have no physical interpretation and were treated as zero. Sample activity was corrected for the activity found in killed controls. All EAAS and microplate reader data processing were done with original Matlab (Mathworks Inc) scripts. Contour maps of activity were generated with Surfer 7 (Golden Software) using the Kriging

interpolation method. Statistical parameters were derived using JMP version 5.1 (SAS Institute Inc).

**Microplate reader**—Enzyme activities also were measured using a Tecan Genios 96-well fluorescence microplate reader. The microplate reader had an excitation/emission filter set of 365/460  $\pm 35$  nm. The detector is 180° from the high energy xenon light source. Three flashes per well were used to excite the fluorophore. The same standard and substrate solutions used in EAAS were used for assays involving the microplate reader. Mixing was done first by rapidly moving a pipette tip when each substrate/standard solution originally was introduced to the well, and again directly before measurement when the entire plate was shaken orbitally for 5 s by the microplate reader at the “normal” setting. For each station, a five-point standard curve was run along with the samples. Each standard fluorescence value used in the microplate reader calculations was the mean of two replicates. The reported activity of a sample measured by the microplate reader was the mean of four replicates. Microplate reader data from the Mullica River, Louisiana shelf, and Hudson estuary use the means of 4 replicates; individual readings (i.e., all replicates were treated as unique samples) were used in the Sargasso Sea and precision studies. Killed controls were run for each sample and their activity subtracted from that of the samples, with the exception of samples taken from the Louisiana shelf.

### Assessment

**EAAS design**—The development of EAAS from a commercially available FIA unit did not overly constrict the design. Fluid flow rate, tubing diameter, length, and geometry are the main physical variables controlling the dynamics of the assay (Narusawa and Miyamae 1995); each parameter was controlled easily.

Sampling from a ship involves certain unique logistics. If the ship's bow or sampling arm rose out of the water, EAAS “sampled” air bubbles, resulting in exceedingly high values measured by the detector. This problem was overcome mostly by use of a small, quick flushing reservoir ( $\sim 30$  mL). The reservoir contained enough water for EAAS to sample fluid from the reservoir should the seawater flow stop, but was shallow enough that new water from the pumping system would be almost instantly available upon return of the flow.

The flow cell had both input and output ferrules attached to the top without tubing extending to the cuvette bottom. A top-filling cuvette increases the chances of introduced fluids not completely mixing before exiting the cuvette. An analysis of the Reynolds number  $\text{Re} = v\rho D/\mu$  with the configuration used in EAAS ( $v \sim 10 \text{ cm s}^{-1}$ ;  $\rho = 0.001 \text{ kg cm}^{-3}$ ;  $D = 0.0508 \text{ cm}$ ;  $\mu = 1\text{e-}5 \text{ kg cm}^{-1} \text{ s}^{-1}$ ) suggests that fluid flow was almost entirely laminar ( $\text{Re} \sim 51$ ). The reaction length ( $\text{RL} = \text{length of tubing required to contain reagent injection prior to mixing}$ ) for EAAS with fluid movement (without dispersion) was  $\text{RL} = 10 \mu\text{L} / 0.002 \text{ cm}^2 \times 2 = 98.7 \text{ mm}$ . Given

**Table 1.** Basic statistics of the EAAS detection limit.

Sampling Area	Enzyme Activity	Detection Limit (nM)*	Standard Deviation (nM)	N†
Louisiana Shelf	Phosphatase‡	0.77	0.42	6
Sargasso Sea	Phosphatase	0.49	0.31	9
Hudson Estuary	Peptidase§	0.32	0.08	6
Tuckerton Estuary	Peptidase	0.54	0	1
All dfMUF-P Samples	Phosphatase	0.60	0.39	15
All Leu-AMC Samples	Peptidase	0.35	0.10	7

\*The detection limit is based on the fluorescence exceeding three times the variation of a distilled water blank.

†N corresponds to the number of standard curves (required for calculating the detection limit) available in each sampling area.

‡Phosphatase detection limits were made using the fluorescent standard dfMUF.

§Peptidase limits were made using AMC.

the height of the cuvette (8.5 mm) and the potential for incomplete mixing of the reaction bolus within the cuvette, it is possible some of the reaction bolus may have been displaced by carrier. This would lower the concentration of substrate or standard in the cuvette, increasing the apparent dilution factor. Evidence for incomplete mixing, either from an overly short mixing coil or top-filling cuvette, is further described below (*see* Slope change). Stirred reaction chambers have been used successfully for mixing (Chen et al. 2006), although switching to a bottom-filling cuvette or insertion of a tube leading to the bottom of the cuvette also would likely increase mixing.

The electrical relay, allowing EAAS to turn the LED on and off, was originally used to mimic the three discrete flashes used by the microplate reader for fluorescence measurements. The relay enabled substrate photolysis from LED illumination to be discounted as a cause of non-linear activity measurements (data not shown).

**Detection limit**—Activity detection limits are both a function of detector sensitivity and incubation time; any positive activity theoretically will provide a detectable increase in fluorescence given a sufficiently long incubation period. The sensitivity of the instrument dictates the incubation time necessary to quantify the reaction rate. To avoid the time-dependence of an activity-based detection limit, the EAAS detection limit was defined purely in terms of minimal observable fluorescence. This approach is valid, as the absolute difference in fluorescence between two time points (the slope) is directly related to activity. The detection limit was calculated for all runs with a unique standard curve (Table 1). The standard deviation of the 0 nM standard was multiplied by three and fit to the standard curve. A one-way analysis of variation (ANOVA) revealed no statistical difference in the detection limit between the Louisiana shelf, Sargasso Sea, and Hudson estuary samples ( $P = 0.094$ ), despite variations in detector integration time and processing of the standards between locations. Similar calculations performed using the microplate reader data resulted in a detection limit of 4–12 nM dfMUF and AMC.

Subtle variations, especially between Louisiana shelf and Hudson estuary samples, may have resulted from differences in colored dissolved matter concentrations and/or tempera-

ture. The fluorescence varied with salinity, exhibiting a maximum fluorescence 1.4 times higher than a similar concentration standard made in distilled water (data not shown). The variations in fluorescence of the standards with salinity precluded using locally sampled seawater for the creation of standard solutions on cruises in estuarine waters. The interpolation between internal standards was used to correct for changes in fluorescence due to variations in salinity, particle concentration (scattering changes), and other variables which may influence fluorescence without directly affecting activity.

The precision of activity measurements by EAAS and the microplate reader was compared in a series of Louisiana shelf plume water samples. The phosphatase activities of 25 EAAS samples were measured as part of a Eularian experiment within the plume of the Mississippi River in 2007. The activities of five consecutive samples within the same patch of plume water (salinity change < 0.1) were measured in five consecutive underway locations. AP activities along the Louisiana shelf in July 2004 were measured by the microplate reader in five different locations with four replicates for each location (20 total activity measurements). EAAS had a mean variation coefficient (standard deviation divided by mean) of 0.13, compared to a value of 0.18 for the microplate reader. Under these experimental conditions (same water, closely spaced measurements in time), the variation coefficient is an indicator of the effect of small scale sample heterogeneity (e.g., sinking particles, turbidity, salinity differences) on activity.

**Measurement mode**—EAAS in stopped-flow continually measured the fluorescence over the course of the incubation. The baseline fluorescence value changed often between samples. Both peak area and peak height values used in continuous-flow measurements could be skewed with non-baseline starting points (Hooley and Dessy 1983). By running in stopped-flow mode, the absolute fluorescence of the starting point of a sample was unimportant compared to the slope of the fluorescence, removing the need to subtract dark current and unhydrolyzed substrate fluorescence values. Changes in fluorescence due to molecular dispersion would not be seen in continuous-flow measurements because the molecular dispersion component is swamped by axial dispersion in continuous-flow (Taylor 1953). This is unfortunately not the case with

stopped-flow, where dispersion within the cuvette can occur without mean fluid flow.

**Flow rates, timing**—In order to minimize sampling time, short distances and fast flow rates between injection point and the detector are desired. These also limit the amount of dispersion and product formation occurring before measurement begins (Hales et al. 2004). EAAS had a very short holding line, extending only the distance from the syringe pump to the multiple position valve and not containing any coils. A small helical coil was placed between the multiple position valve and the detector to increase the mixing between seawater and substrate without spreading the reaction mixture in the tubing overly or increasing the sample analysis time drastically. The flow rate to the detector was purposefully kept slow to maximize axial dispersion despite the undesired decrease in sampling rate. Additionally, some processing speed was sacrificed for increased resolution in the mixing and reaction processes.

Overall sampling rates could be increased by changing some key features of EAAS. The time required to run the standard curve could be reduced by switching fluorescence measurements of the standards to a continuous-flow detection method, as peak fluorescence from a continuous-flow assay was set equal to the stopped-flow value by centering the reaction bolus. The substrate baseline also could be run in continuous-flow mode because only the maximum fluorescence (not a slope) is used in the data analysis. Internal standards potentially could be run in continuous-flow if the fluorescence was measured as the difference between individual peak baselines (rather than the blank value at the start of the run) and peak apices, so as to avoid errors due to inter-sample variations in the baseline. The number of wash cycles after sample and standard measurements probably could be reduced as a return to baseline fluorescence was observed with only the ~2 mL residual fluid from a sample.

**Slope change**—The hydrolysis reactions in EAAS produce a linear increase in fluorescence over the time scales of EAAS incubations (Gee et al. 1999); deviations from linearity are indications of aberrations in the reaction. Incomplete mixing prior to measurement may give temporarily higher or lower fluorescence values than the mean depending on the concentration difference between heterogeneous pockets of reagent and the hypothetical homogenous solution and localization within the cuvette (i.e., higher if passing in front of the window and lower if leaving). Particles also could affect fluorescence variably (with particle flux affecting fluorescence over time), increasing the signal through increased scatter of incident light and localization of the hydrolysis reactions to particle surfaces, or decreasing fluorescence through increased attenuation.

Samples with low, positive activity often would create a checkmark shape (Fig. 3). Samples with higher activities had correspondingly steeper initial decreases in activity, as well as higher fluorescence by the end of the run. It seems likely that the specific activity of ectoenzymes in the solution during the short incubation period did not change, despite the change in

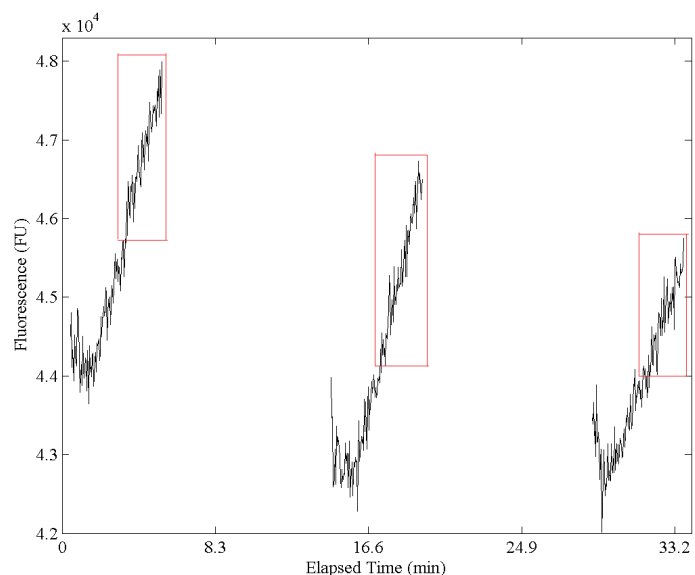


**Fig. 3.** Section of Hudson estuary data collected by EAAS displaying evidence of dispersion within the cuvette. Only the final one-third of the measured fluorescence (red boxes) was considered when calculating slopes. A linear least-squares regression was fit to these data subsets to arrive at sample slope.

slope seen in the graph. Rather, the two-part slope is probably a change in the spatial distribution of activity, consistent with a process where a concentrated pocket of substrate/standard is injected in the cuvette and diffuses into a homogenous solution. Hence, the final one-third of the data used as the “true” (post-diffusion or settling) activity slope should be representative of the entire incubation.

Noticeable dispersion within the cuvette would likely be eliminated if the reaction bolus was well-mixed prior to delivery to the flow cell. However, reaching the required degree of mixing through dispersion in laminar flow is difficult, and complete replacement of fluid within the flow cell is required to remove measurable dispersion effects, unless homogenization within the cuvette is allowed. Bottom-filling the cuvette is perhaps the most effective method available for EAAS. In-line filtering of seawater samples to remove particles did not appear to be advisable. In regions of high turbidity, the filter could become clogged resulting in increased pressure within the sampling line and possibly bursting cells. In addition, some large phytoplankton can contribute to ectoenzyme activity (Hoppe 2003); filters capable of removing these particles would decrease bulk activity measurements.

**Comparison with microplate reader**—A comparison was run between EAAS and a fluorescence microplate reader set to EAAS conditions using the peptidase substrate Leu-AMC (Fig. 4). Samples from a variety of salinities were taken along the Mullica River near the Rutgers University marine research station and the LEO-15 ocean observatory. Salinity varied from 1.6 to 30. Samples ( $n$  = number of discrete samples) were taken from the bottom of the river ( $n$  = 2), near exposed aquatic vegetation

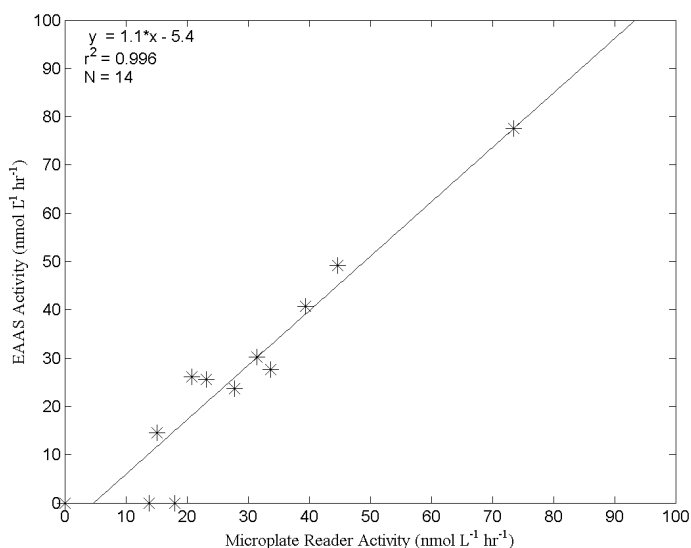


**Fig. 4.** EAAS versus microplate reader peptidase activities. Samples were run simultaneously by EAAS and a fluorescence microplate reader. One additional point at (Microplate = 342.05, EAAS = 380.79) is out of range of the graph and not shown, but was included in the regression. The correlation coefficient decreases slightly to 0.92 when this point is removed. One data point was omitted due to a non-linear slope ( $r < 0.9$ ) in EAAS data.

( $n = 3$ ), and open surface water ( $n = 9$ ), and run 3 h after initial collection. Leu-AMC activities were calculated using a 5 min incubation time, paying special attention to mixing the microplate wells thoroughly and reducing the delay between processing a sample with EAAS and the microplate reader. EAAS activity was regressed against activity measured by the microplate reader with the resulting linear least-squares equation: EAAS Activity =  $1.1 \times$  Microplate Activity – 5.4. The  $r^2 = 0.996$ ,  $n = 14$ . One data point with a non-linear slope ( $r < 0.9$ ) was excluded from EAAS activity data. (Sample slopes from the Louisiana shelf, Sargasso Sea, and Hudson estuary were not analyzed for linearity due to the high sample numbers.) The correlation coefficient decreased slightly ( $r^2 = 0.92$ ) when the highest activity point was removed from the calculation. The two points with positive microplate reader activity and zero EAAS activity both originate from areas of the river with very high suspended sediment (river bottom and a muddy patch of grass). The high suspended sediment concentration and associated scattering, attenuation, and/or enzyme-attached particles may have contributed to the differences in activity between the instruments.

**Field validation—Gulf of Mexico.** EAAS was deployed in the Louisiana shelf area of the Gulf of Mexico from 16 July 2004 – 20 July 2004 aboard the R/V Pelican. The cruise track zig-zagged between Mississippi River plume water (salinity 10) and offshore seawater (salinity 34). As this area is known to be hypereutrophic (Lohrenz et al 1997; Rabalais et al. 2002) with high AP activities (Ammerman and Glover 2000; Sylvan et al 2006), EAAS incubation times using dfMUF-P were set at 5 min.

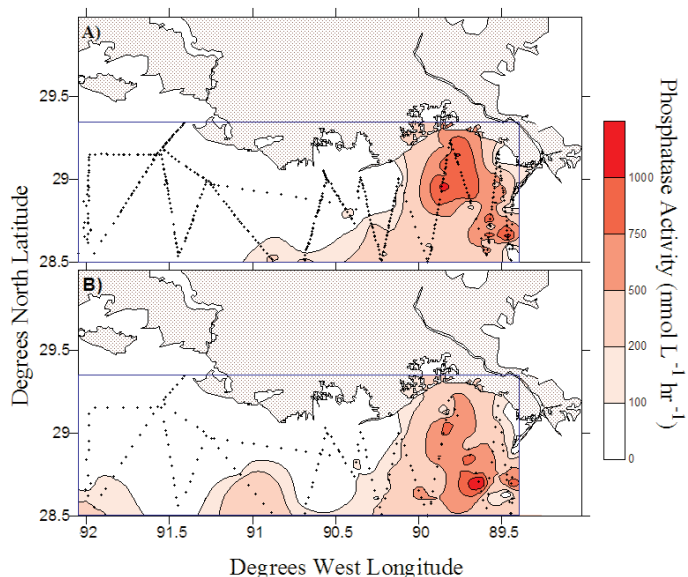


**Fig. 5.** Contour maps of AP activity. The black dots are sample positions, determined by matching the ship cruise track to the start time of each EAAS sample. The blue line demarcates contoured area. Map A was made from EAAS data ( $n = 344$ ). Map B was created from the less densely sampled fluorescence microplate reader data ( $n = 173$ ).

EAAS sampled every 11 min with  $\sim 1.5$  h data gaps occurring between runs in order to wash EAAS and create new standard curves. Samples to be analyzed on the microplate reader were acquired from surface waters approximately every 30 min, although most samples were run hours after their acquisition. The incubation time for activities measured on the microplate reader was 45 min.

The contour plot of AP activity from EAAS data (Fig. 5a) shows a clear trend of highest activity west of the Mississippi River mouth and decreasing activity further west. This is attributed to the high concentration of nitrogen in the Mississippi River outflow, thereby providing enough excess nitrogen to the system that it experiences phosphorus limitation (Sylvan et al. 2006). Two main areas of high activity are seen, generally flanking Southwest Pass. The direction of the coastal current is known to vary seasonally with the dominant western direction briefly interrupted by summer easterly currents (Hitchcock et al. 1997). Interestingly, there was no activity around the Atchafalaya River mouth. The regions furthest away from Southwest Pass maintained low activities.

The contour map of AP activity from microplate reader data (Fig. 5b) is similar in most respects to that of EAAS. Activity was highest near the Mississippi River mouth, and decreased with distance, although the area of highest activities measured by EAAS was larger than the area measured by the microplate reader. As with the map of EAAS data, activity was seen flanking Southwest Pass. No enzyme activity was seen in the area of Atchafalaya River influence or the open water at the far west of the cruise track.

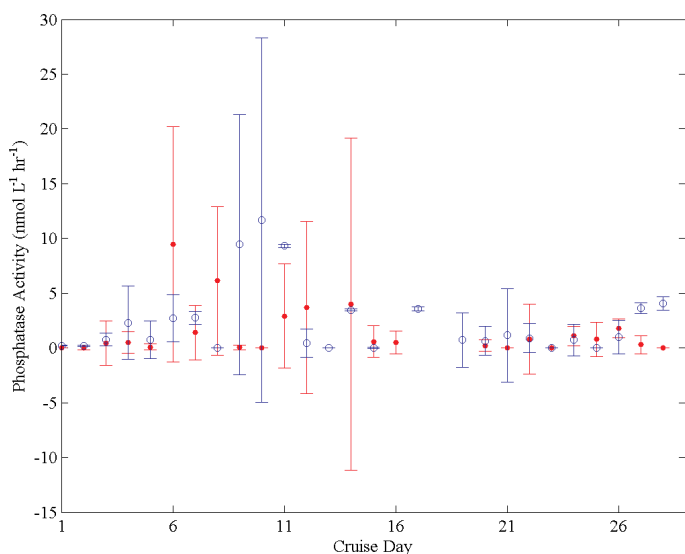


**Fig. 6.** Sargasso Sea time series of AP activity measured by both EAAS (red) and the microplate reader (blue). Error bars are standard deviation. The beginning of the time series is 17 February 2005. Activities are averaged per day. Data gaps occurred during periods when weather prevented CTD deployment and/or shut off internal seawater flow to EAAS. A major storm event occurred from 22 February 2005 until 8 March 2005 (cruise day 6–20). EAAS measured 579 samples over the cruise, with 256 measurements (70 discrete) made using the microplate reader.

The differences in activities between EAAS and the microplate reader, especially considering the strong relationship found in the Tuckerton, New Jersey samples, are worth discussing. The comparison experiment measured activity of the same water sample after an identical delay between sample acquisition and processing. This is in contrast to the Louisiana samples in which water samples, although occasionally taken in proximity to EAAS samples, were neither identical nor processed after the same delay. Spatial differences and sample confinement in bottles (in the case of microplate reader samples) are expected to cause variation in enzyme activities. Instrument sensitivity also may play a role in producing systematic differences in very low activity regions where the detection limit partially defines measurable activity.

**Sargasso Sea.** The Sargasso Sea is a phosphorus-deficient oligotrophic environment with unusually high nitrogen to phosphorus ratios (Cotner et al. 1997; Ammerman et al. 2003). EAAS was deployed on a month-long cruise (17 February 2005 – 15 March 2005) aboard the R/V *Oceanus*, ranging up to 150 km away from Bermuda. The initial and final days of the cruise consisted of fair weather, a sharp contrast to the bulk of the cruise (22 February 2005 – 8 March 2005, cruise days 6–20) where wind-driven mixing (with an associated 300 m mixed layer depth) and rain dominated. EAAS used 20 min incubations of dfMUF-P, although the microplate reader incubation time was set at 2.5 h for both dfMUF-P and Leu-AMC activities.

AP activity measured by EAAS began very low, increased to a maximum of  $\sim 10$  nmol L<sup>-1</sup> hr<sup>-1</sup> on the sixth day of the cruise,

and generally maintained higher activities until the end of the time series (Fig. 6). Activity, averaged by day, was mostly very low with a mean activity of 1.5 nmol L<sup>-1</sup> hr<sup>-1</sup>. The average activity is in good agreement with values previously reported for the Sargasso Sea (Ammerman et al. 2003), including experiments using much longer incubation times. The higher EAAS activities, usually associated with late spring/early summer activities (Ammerman et al. 2003), may reflect the extremely stormy weather, conditions under which enzyme activity measurements are not routinely made. The large number of samples per day, in the relatively constant environment (for each day) of the Sargasso Sea, kept the average standard error within  $\sim 11\%$  of the daily mean. However, although precautions were taken to eliminate data inconsistencies due to air bubbles (large waves would often lift the seawater intake out of the water), some of the larger scatter, especially between 22 February 2005 – 2 March 2005 (cruise days 6–14), is likely a reflection of this sort of sampling error.

Most of the samples for the microplate reader were taken from CTD casts, although some samples from the ship's uncontaminated seawater system also were run. AP activity measured by the microplate reader had a similar pattern as EAAS data, although activities are generally higher than EAAS values. Coupled with data gathered in the Louisiana shelf, this indicates that a simple systematic difference between the two instruments does not account fully for discrepancies in activity. Unlike the Louisiana shelf and Hudson estuary, the uniformity of the water the ship sampled each day allowed each microplate reader replicate to be treated as a unique sample for the purposes of calculating the mean daily activity and standard deviation. Variations in activity between the instruments are likely a result of differences between the instrument settings (incubation time for very low activities, detector parameters), small scale differences in sampling location (EAAS from the ship intake in the bow, microplate reader from the CTD off the starboard side), or from diel variations in activity captured by EAAS but not available to the microplate reader due to a lower sampling frequency.

**Hudson River estuary.** The Hudson River estuary experiences eutrophication from nutrient input in the New York/New Jersey area (Taylor et al. 2003). During the 8 April 2005 – 20 April 2005 cruise aboard the RV *Oceanus*, EAAS sampled the ship's uncontaminated seawater system in the dry lab for peptidase using Leu-AMC as the substrate and a 5 min incubation. The cruise track included the Hudson River plume, sites offshore from the coast of Long Island, and oscillations in and out of the plume water down the New York/New Jersey coast.

The oscillating data (Fig. 7) between 17 April 2005 and 18 April 2005 occurred while traveling down the coast, making excursions out to sea and then back to shore. The first two major peaks in peptidase activity corresponded to periods when the ship was close to the shore; activity lows implied ship positions further out to sea in higher salinity water. The inflection points of activity peaks occurred at different levels

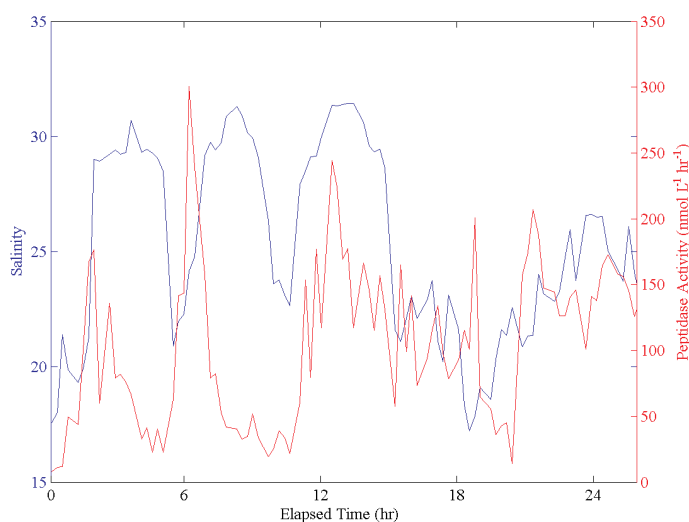


**Fig. 7.** Section of Hudson River estuary salinity and peptidase activity time course. The beginning of the time series is 2215 h on 16 April 2005. The red line and right red axis corresponds to EAAS peptidase activity. The blue line and left blue axis corresponds to salinity as measured by the ship's flow-through salinometer. Oscillations in these parameters occurred as the ship moved in and out of the Hudson River plume along the New Jersey coast.

of activity, a result explained by water of different age and degree of nutrient use being sampled down the coast. In contrast, activity lows were at approximately the same level, an expected result for waters with the same nutrient and biomass load. Activity peak widths were significantly smaller (~3.5 h) and often preceded those of salinity. Beginning the 12<sup>th</sup> h of the time series, activity and salinity changes occurred in phase and in the same direction. The switch in the activity-salinity relationship seems related to an entrainment of old surface water coincident with the head of Hudson Canyon. The automated nature of EAAS allowed detection of in-shore/off-shore variations of a faster frequency than similar microplate measurements could be made, as well as identifying a major change in the activity-salinity relationship.

## Discussion

Manual ectoenzyme assays have been performed with a single sample fluorometer for decades and with fluorescence microplate readers for around a decade. However, the development of EAAS marks the first time FIA has been used to automate measurements of enzyme activities in natural marine systems. Compared to other techniques, ectoenzyme assays measured by EAAS required minimal user intervention and had much higher sampling rates. As a result, the effort and cost of a technician is drastically reduced for enzyme assays using EAAS.

EAAS activities occasionally differed from those measured by the microplate reader, although spatial and temporal trends appear similar. Differences in instrument sensitivity, mixing, elapsed time from sample acquisition to measurement, incubation time, numbers of discrete samples

measured per day, detector configuration (EAAS measures fluorescence 90° from excitation source, the microplate reader at 180°), emission filter cut-offs, and detector parameters (flash frequency, integration time) all could potentially contribute to disparity in measured enzyme activities. Special attention to duplicating measurement parameters was needed to align microplate reader activities with that of EAAS. Repeatability of experimental conditions is mandatory for field work comparing enzyme activities on either spatial or temporal scales. Automation of the substrate injection, mixing, and incubation is hence the preferred methodology for replicate sampling, as seen in the lower variation coefficient of EAAS data.

In both the Louisiana shelf and Hudson River estuary cruises, highest activity was found at intermediate salinities. Paired with the brief and drastic increases in enzyme activity seen in the Sargasso Sea under fairly extreme sampling conditions, EAAS demonstrates the utility of automated and continuous ectoenzyme measurements for the exploration of biogeochemical systems.

The automated nature of EAAS makes it ideal for surface mapping of large areas. Minimal operator intervention is required and the same operator can run the machine continuously for extended periods. Several existing environmental studies lend themselves well to automated enzyme activity measurements. The annual zone of hypoxia along the Louisiana shelf in 2004 was approximately 15,000 km<sup>2</sup>, near the long-term average (<http://www.gulfhypoxia.net>). Complete manual coverage of the large spatial extent of the shelf can strain human resources, and potentially could miss important features. Automated activity measurements are also ideal for projects incorporating long transects similar to WOCE (World Ocean Circulation Experiment) lines. Automated sampling and processing is preferred due to the long duration of these cruises, the emphasis on identifying a gradient of biological and chemical parameters along these transects, and the associated requirement for analytical consistency. It would also be useful for high resolution temporal studies at a single location. EAAS could be mounted on a pier, shore-based observatory, or any other fixed site with suitable infrastructure. Continuous sampling of enzyme activity can allow analyses of variations based on river flow, nutrient concentrations, tidal cycles, cloud cover, or other variables. Studies looking at contaminant remediation also can be assisted by automated enzyme data. By its nature, ectoenzyme activity is a measure of organic matter turnover. Hence, high density activity data can be used as an indicator of organic matter use. This may be of particular management interest when looking at natural rates of contaminant hydrolysis. High resolution contour maps and time-series studies of ectoenzyme activities in eddies, localized upwellings and downwellings, blooms, and river plumes may be used to understand and predict the biogeochemical changes in these and other aquatic environments.

## References

- Ammerman, J. W., and W. B. Glover. 2000. Continuous under-way measurement of microbial ectoenzyme activities in aquatic ecosystems. *Mar. Ecol. Prog. Ser.* 201:1–12.
- — —, R. R. Hood, D. A. Case, and J. B. Cotner. 2003. Phosphorus deficiency in the Atlantic: an emerging paradigm in oceanography. *Eos Trans.* 84:165–170.
- Beardall, J., E. Young, and S. Roberts. 2001. Approaches for determining phytoplankton nutrient limitation. *Aquat. Sci.* 63:44–69.
- Chen, Y., A. D. Carroll, L. Scampavia, and J. Ruzicka. 2006. Automated method, based on micro-sequential injection, for the study of enzyme kinetics and inhibition. *Analyt. Sci.* 22:9–14.
- — —, and J. Ruzicka. 2004. Accelerated micro-sequential injection in lab-on-valve format, applied to enzymatic assays. *Analyst* 129:597–601.
- Christian, J. R., and D. M. Karl. 1995. Bacterial ectoenzymes in marine waters: activity ratios and temperature responses in three oceanographic provinces. *Limn. Oceanogr.* 40:1042–1049.
- Chrost, R. J. 1991. Environmental control of the synthesis and activity of aquatic microbial ectoenzymes, p. 29–59. *In* R. J. Chrost [ed.], *Microbial enzymes in aquatic environments*. Springer.
- — —, and W. Siuda. 2002. Ecology of Microbial Enzymes in Lake Ecosystems, p. 35–72. *In* R. G. a. D. Burns, R.P. [ed.], *Enzymes in the Environment*. Marcel Dekker, Inc.
- Cotner, J. B., J. W. Ammerman, E. R. Peele, and E. Bentzen. 1997. Phosphorus-limited bacterioplankton growth in the Sargasso Sea. *Aquat. Microb. Ecol.* 13:141–149.
- Delmas, D., and M. J. Garet. 1995. SDS-preservation for deferred measurement of exoproteolytic kinetics in marine samples. *J. Microb. Methods* 22:243–248.
- — —, C. Legrand, C. Bechemin, and C. Collinot. 1994. Exoproteolytic activity determined by flow injection analysis: its potential importance for bacterial growth in coastal marine ponds. *Aquat. Living Resour.* 7:17–24.
- Gee, K. R., Sun, W.-C., Bhalgat, M.K., Upson, R.H., Klaubert, D.H., Latham, K.A., and Haugland, R.P. 1999. Fluorogenic substrates based on fluorinated umbelliferones for continuous assays of phosphatases and beta-galactosidases. *Analyt. Biochem.* 273:41–48.
- Hales, B., A. Van Geen, and T. Takahashi. 2004. High-frequency measurement of seawater chemistry: flow-injection analysis of macronutrients. *Limn. Oceanogr.: Methods* 2:91–101.
- Hitchcock, G. L. Wiseman, W.J., Boicourt, W.C., Mariano, A.J., Walker, N.D., Nelson, T.A., and Ryan, E. 1997. Property fields in an effluent plume of the Mississippi River. *J. Mar. Sys.* 12:109–126.
- Hooley, D. J., and R. E. Dessy. 1983. Continuous flow kinetic techniques in flow injection analysis. *Analyt. Chem.* 55:313–320.
- Hoppe, H-G. 1993. Use of fluorogenic model substrates for extracellular enzyme activity (EEA) measurement of bacteria, p. 423–431. *In* P. F. S. Kemp, B.F. Sherr, E.B. Cole, J.J. [ed.], *Handbook of methods in aquatic microbial ecology*. Lewis Publishers.
- — —. 2003. Phosphatase activity in the sea. *Hydrobiol.* 493:187–200.
- Huston, A. L., and J. W. Deming. 2002. Relationships between microbial extracellular enzymatic activity and suspended and sinking particulate organic matter: seasonal transformations in the North Water. *Deep-Sea Res. Part II-Top. I Stud. Oceanogr.* 49:5211–5225.
- Jarvinen, M., K. Salonen, J. Sarvala, K. Vuorio, and A. Virtanen. 1999. The stoichiometry of particulate nutrients in Lake Tanganyika- implications for nutrient limitation of phytoplankton. *Hydrobiol.* 407:81–88.
- Kirchman, D. L., A. I. Dittel, S. E. Findlay, and D. Fischer. 2004. Changes in bacterial activity and community structure in response to dissolved organic matter in the Hudson River, New York. *Aquat. Microb. Ecol.* 35:243–257.
- Lohrenz, S.E., Fahnenstiel, G.L., Redalje, D.G., Lang, G.A., Chen, X.G., and Dagg, M.J. 1997. Variations in primary production of northern Gulf of Mexico continental shelf waters linked to nutrient inputs from the Mississippi River. *Mar. Ecol. Prog. Ser.* 155:45–54.
- Martinez, J., and F. Azam. 1993. Periplasmic aminopeptidase and alkaline phosphatase activities in a marine bacterium: implications for substrate processing in the sea. *Mar. Ecol. Prog. Ser.* 92:89–97.
- Marx, M. C., M. Wood, and S. C. Jarvis. 2001. A microplate fluorimetric assay for the study of enzyme diversity in soils. *Soil Bio. Biochem.* 33:1633–1640.
- Narusawa, Y., and Y. Miyamae. 1995. Evidence of axial diffusion accompanied by axial dispersion with zone circulating flow-injection analysis data. *Analytica Chimica Acta* 309:227–239.
- Perry, M. J. 1972. Alkaline phosphatase activity in subtropical Central North Pacific waters using a sensitive fluorometric method. *Mar. Biol.* 15:113–119.
- Rabalais, N. N., R. E. Turner, Q. Dortch, D. Justic, V. J. Bierman, and W. J. Wiseman. 2002. Nutrient-enhanced productivity in the northern Gulf of Mexico: past, present and future. *Hydrobiol.* 475:39–63.
- Ruzicka, J. 2000. Flow Injection: From Beaker to Microfluidics. *Analytical Chem.* 72:212A–217A.
- Sebastian, M., J. Aristegui, M. F. Montero, J. Escanez, and F. X. Niell. 2004. Alkaline phosphatase activity and its relationship to inorganic phosphorus in the transition zone of the North-western African upwelling system. *Prog. Oceanogr.* 62:131–150.
- Soderstrom, J. 1996. The significance of observed nutrient concentrations in the discussion about nitrogen and phosphorus as limiting nutrients for the primary carbon flux in coastal water ecosystems. *Sarsia* 81:81–96.

- Stepanauskas, R., H. Edling, and L. J. Tranvik. 1999. Differential dissolved organic nitrogen availability and bacterial aminopeptidase activity in limnic and marine waters. *Microb. Ecol.* 38:264–272.
- Sylvan, J. B., Q. Dortch, D. M. Nelson, A. M. Brown, W. Morrison, and J. W. Ammerman. 2006. Phosphorus limits phytoplankton growth on the Louisiana shelf during hypoxia formation. *Environ. Sci. Technol.* 40:7548–7553.
- Taylor, G. 1953. Dispersion of soluble matter in solvent flowing slowly through a tube. *R. Soc. Lond. Ser. A Math. Phys. Sci.* 219:186–203.
- Taylor, G. T., J. Way, Y. Yu, and M. I. Scranton. 2003. Ectohydrolase activity in surface waters of the Hudson River and western Long Island Sound estuaries. *Mar. Ecol. Prog. Ser.* 263:1–15.

*Submitted 18 June 2007*

*Revised 21 August 2007*

*Accepted 31 August 2007*